# Rollable metamaterial screen for magnetic resonance coupling-based high-efficiency wireless power transfer

Woosol Lee 🔵 and Yong-Kyu Yoon

Department of Electrical and Computer Engineering, University of Florida, Gainesville, FL, USA

## Abstract

This paper presents a rollable metamaterial screen for high-efficiency wireless power transfer (WPT) system based on magnetic resonance coupling, which operates at 4.5 MHz. The rollable metamaterial screen with a fully expanded area of 750 mm × 750 mm is located in the middle between transmitter and receiver coils and focuses the magnetic field and, by such a way, significantly improves power transfer efficiency (PTE). The metamaterial screen can be rolled up, e.g. onto the ceiling when it is not used, and thus does not require any designated space for the screen saving space. A WPT system with the rollable metamaterial screen is designed, fabricated, and characterized. Improved PTE is qualitatively and quantitatively verified by light bulb experiments and vector network analyzer measurements. The PTE of the WPT system with the metamaterial screen increases from 36 to 58.52% and 10.24 to 31.36% for the distances between the transmitter and receiver coils 100 and 150 cm, respectively. The effects of lateral and angular misalignments on the PTE of the WPT system are also studied. Obtained results show that the rollable metamaterial screen improves the PTE even at the misaligned condition.

## Introduction

Research and development activities in wireless power transfer (WPT) area are actively executed because of the high demand for wireless charging in the modern commercial electronics. Most of current WPT systems have limited power transfer distance (PTD) and efficiency as they adopt the inductive coupling approach. In order to extend the power transfer capability to mid-range distances, the magnetic resonance coupling (MRC) approach can be utilized. This method, first introduced by Tesla, increases the PTD by using high-$Q$ resonant coils [1]. To enhance the power transfer efficiency (PTE) of the MRC-based WPT system, the transmitter and receiver coils should be designed to resonate at the same frequency. However, the increase of the PTD decreases the magnetic coupling between the transmitter and receiver coils, which results in the PTE decreases and limits the PTD of the MRC-based WPT system [2]. Furthermore, the PTE of the WPT system heavily depends on the misalignment between the transmitter and receiver coils. Due to these challenges, the practical applications of the MRC-based WPT in commercial electronic devices are also limited.

Researchers have reported that metamaterials can be utilized for improving the PTE of the WPT systems [3–8]. Metamaterials are artificially engineered materials that show uncommon electromagnetic properties, such as evanescent wave amplification and negative refractive characterisics, which could be exploited for the enhancement of PTE [9]. The earlier investigations of metamaterials are done in 1968 by Veselago, who introduced the substances with the simultaneous negative values of permittivity and permeability which induce the negative refractive property and focusing property of metamaterials [10]. In 2000, Pendry demonstrated that a negative refractive metamaterial slab can focus the electromagnetic waves and amplify the evanescent waves, and therefore it can be utilized to fabricate a "perfect lens" [11]. Concerning the WPT systems, Urzhumov and Smith provided a theoretical analysis of the negative refractive metamaterial lenses for improving the PTE [12]. Later, Wang *et al.* introduced the WPT system with the negative refractive metamaterial slab effectively enhancing the PTE [3].

The metamaterial structures in these previous works have been inserted between the transmitter and receiver coils to increase the PTE of the WPT system [3, 4]. However, those metamaterial structures have been bulky and volumetric, three-dimensional (3D), and thick PCB-based structures with the negative refractive properties [3–6]. It has been reported recently that the negative refractive property could be realized without using such bulky structures [7, 8]. In fact, since the thick substrate could add an additional substrate loss, a thinner metamaterial layer should be preferably used if possible for these purposes. Also, the WPT systems need to satisfy the common technology trend to be of reduced size, weight, and
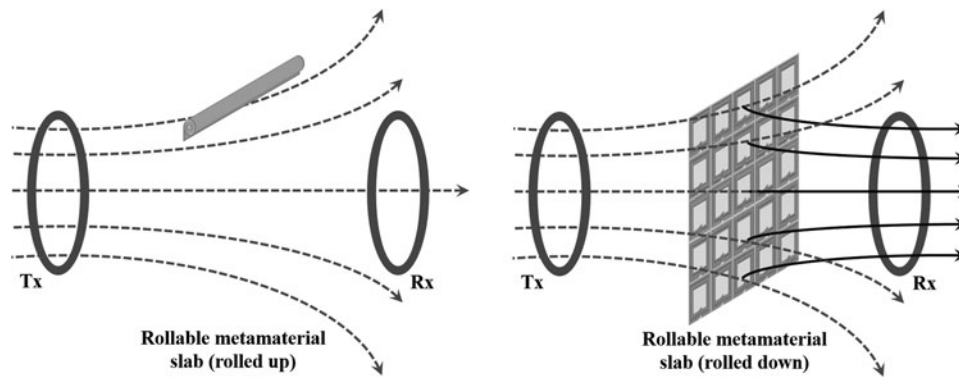
**Fig. 1.** Conceptual configuration of the WPT system with the rollable metamaterial screen.
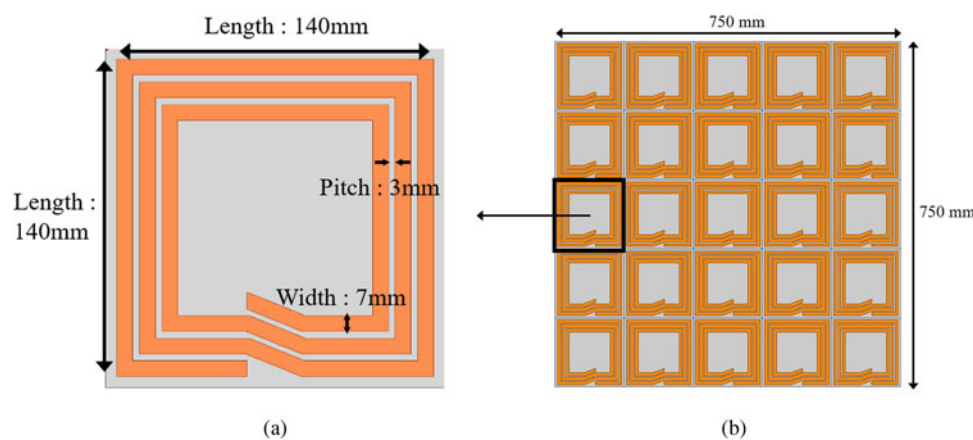


**Fig. 2.** Schematic configuration of: (a) Single metamaterial unit cell. (b) Rollable metamaterial screen.

consumed power (SWaP). Especially, for the efficient usage of the space, the modern consumer electronics should have a possibility for changing their form factors or able to be deformed, rolled, and folded, such as rollable TVs and foldable smartphones without compromising the performance of their electronic systems while still enhancing their portability. It would be interesting to watch out if the above mentioned technological trend can be implemented in designing and developing the modern WPT systems.

In this study, it is proposed, for the first time to our best knowledge, a rollable metamaterial screen built on a flexible polyethylene substrate for using in the high-efficient WPT systems based on a four-coil system consisting of a source coil, a transmitter coil, a receiver coil, and a load coil. The rollable metamaterial screen is placed in the middle between the transmitter and receiver coils to enhance the PTE. The rollable metamaterial screen can be rolled up or rolled down as needed (Fig. 1), it enables users to utilize the space flexibly. For example, the rolled-up screen can be placed on a ceiling and only when an efficient WPT is needed, the screen can be rolled-down. By such a way, the PTE of the WPT system can be enhanced without using a permanently placed metamaterial structure. The proposed rollable metamaterial screen is built on a thin slab so that the PTE is additionally improved by decreasing the power losses occurring within the large and thick structures of the metamaterial slabs. The WPT system with the rollable metamaterial screen shows the PTE improvement by a factor 3.06 at a transfer distance 150 cm as compared with the same WPT system without the

metamaterial screen. We experimentally verified the effectiveness of the WPT system in qualitative light bulb experiments and quantitative vector network analyzer measurements.

## Design and analysis of the rollable metamaterial screen

There are some challenges affecting the design of the rollable metamaterial screen. Even though the metamaterial screen can improve the PTE of the WPT system, the metamaterial structure itself introduces additional power losses, which should be minimized. In order to obtain low power losses within a thin artificial metamaterial, a square spiral resonator, which is easy to fabricate and reproduce, is used as a metamaterial unit cell. Previous study shows that this square spiral resonator is preferred to a split-ring resonator in terms of the $Q$-factor [13], which means that the square spiral resonator has lower power losses than the split-ring resonator does.

As shown in Fig. 2(a), the square spiral resonator, which is a metamaterial unit cell, is fabricated on a flexible polyethylene substrate ($\varepsilon_r = 2.25$) which has a thickness of 0.0762 mm. The metamaterial unit cell has three turns, with a copper strip width 3 mm and a pitch between neighboring strips 3 mm. The length of the unit cell is 140 mm. The metal (copper) thickness is 0.0799 mm. In order to operate at the resonant frequency of the WPT system, a capacitor is connected to the endpoint of each unit cell. In addition, each turn of each unit cell is connected to the following turn through the bend. It enables one to optimize

the space and minimize the distance between the endpoints. Since the capacitor is connected between the endpoints, unnecessary inductance of the connecting line is minimized.

As shown in Fig. 2(b), the rollable metamaterial screen consists of $5 \times 5$ metamaterial unit cells. The gap between the neighboring metamaterial unit cells is 10 mm. The total size of the rollable metamaterial screen is 750 mm $\times$ 750 mm. The total thickness of the rollable metamaterial screen is 0.16 mm which is much thinner than the thickness of the previously reported metamaterial slab (1.2, 1.6, and 23.3 mm) [3–5]. This rollable metamaterial screen is flexible and easy to roll as it has a thin conductor and substrate layers.

High Frequency Structure Simulator (HFSS, Ansys Inc., Canonsburg, PA, USA) is utilized to simulate a full 3D structure of the proposed metamaterial unit cell. The refractive index, $n$, and the value of the relative permeability, $\mu_r$, are calculated from the HFSS simulation results ($S_{11}$, $S_{21}$) by using the standard retrieval methods, which associates the S-parameters with the refractive index and the relative permeability [14–16] as follows:

$$S_{11} = \frac{R_{01}(1 - e^{i2nk_0d})}{1 - R_{01}^2 e^{i2nk_0d}}, \tag{1}$$

$$S_{21} = \frac{(1 - R_{01})e^{i2nk_0d}}{1 - R_{01}^2 e^{i2nk_0d}}, \tag{2}$$

$$z = \pm \sqrt{\frac{(1 + S_{11})^2 - S_{21}^2}{(1 - S_{11})^2 - S_{21}^2}}, \tag{3}$$

$$e^{ink_0d} = \frac{S_{21}}{1 - S_{11}(z - 1/z + 1)}, \tag{4}$$

$$n = \frac{1}{k_0d}\{[[[\ln(e^{ink_0d})]''] + 2m\pi] - i[\ln(e^{ink_0d})]'\}, \tag{5}$$

$$\mu_r = nz, \tag{6}$$

where $S_{11}$ and $S_{21}$ are reflection and transmission S-parameters; $(\cdot)'$ and $(\cdot)''$ denote the real part and imaginary part of the complex numbers, respectively; $R_{01}$ is $z - 1/z + 1$; $n$ is the refractive index; $k_0$ is the wavenumber; $d$ is the maximum thickness of the slab; $z$ is the impedance; $m$ is the integer related to the branch index of $n'$. Equation (3) is obtained by inverting equations (1) and (2), and equation (5) is determined by equation (4). Finally, the value of the relative permeability can be calculated by equation (6) using equations (3) and (5).

Results of calculations show (Fig. 3) that the real part of the relative permeability defines the refraction index which determines how much the direction of the magnetic field is refracted when entering the metamaterial screen. This refraction would be described using Snell's law of refraction, $n_1\sin\theta_1 = n_2\sin\theta_2$, where $\theta_1$ and $\theta_2$ are the angles of incidence and refraction, respectively, of the electromagnetic field crossing the boundary between two materials with refractive indices $n_1$ and $n_2$. The imaginary part of the relative permeability is defined by the magnetic loss tangent which reflects the power losses. It means that the metamaterial screen with the large negative refraction index focuses the magnetic field more effectively in the preferred direction. However, when the negative refraction index becomes even larger, the operating frequency is shifted closer to the resonant
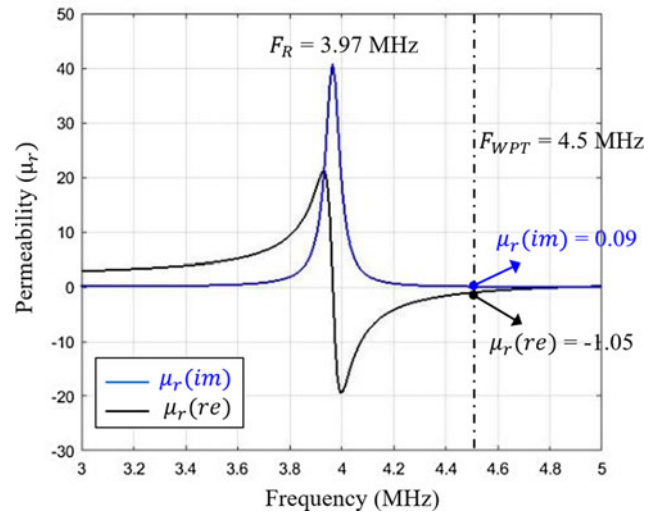


**Fig. 3.** Calculated relative permeability of the rollable metamaterial screen.

frequency of the unit cell, which causes larger power losses. Therefore, both the real part and the imaginary part of the relative magnetic permeability are the critical design factors. The proposed WPT system operates at a resonant frequency 4.5 MHz. The resonant frequency of the metamaterial unit cells is 3.97 MHz, and its real value of the relative permeability is −1.05 at 4.5 MHz which means it has a negative refraction index value of −1. The imaginary value of the relative permeability is 0.09, which means it is designed to have relatively low power losses. The imaginary and real parts of the calculated relative permeability of the rollable metamaterial screen are shown in Fig. 3.

## Fabrication of the rollable metamaterial screen and four-coil wireless power transfer system

The rollable metamaterial screen is fabricated on a flexible and thin polyethylene substrate which has a thickness of 0.0762 mm, as shown in Fig. 4. In order to have a negative refraction property at 4.5 MHz, two ceramic capacitors (470 pF, RCE5C2A471J0A2H03B, Murata) are connected to each unit cell in parallel. This rollable metamaterial screen is flexible and easy to roll as it has a thin conductor and substrate layers.

The four-coil WPT system is fabricated to verify the effectiveness of the rollable metamaterial screen. As shown in Fig. 5, this WPT system consists of a source coil, a transmitter (Tx) coil, a receiver (Rx) coil, and a load coil. The source and load coils have a single turn with diameter 400 mm. The Tx and Rx coils have 12 turns, a turn-to-turn pitch 1 cm, and an outer diameter 60 cm. All coils are fabricated using a 2.588 mm diameter copper wire. The resonant frequency of this four-coil WPT system is 4.5 MHz. Equivalent circuit models of the four-coil system with and without the metamaterial screen are shown in Figs 6(a) [17] and 6(b), respectively. The parameters of each coil are described by $R_iL_iC_i$ models ($i = 1 - 4$ and $U_1 - U_n$). The coupling coefficients between two coils are represented by coefficients $k_{12}$, $k_{23}$, and $k_{34}$, while coefficients $k_{13}$, $k_{14}$, and $k_{24}$ are neglected as the corresponding distances are much larger and the coupling factors are much smaller than ones of the first group. In addition, $k_{2U_i}$ and $k_{3U_i}$ are included into the model when the metamaterial screen is used ($i = U_1 - U_n$). In order to obtain the high PTE, the
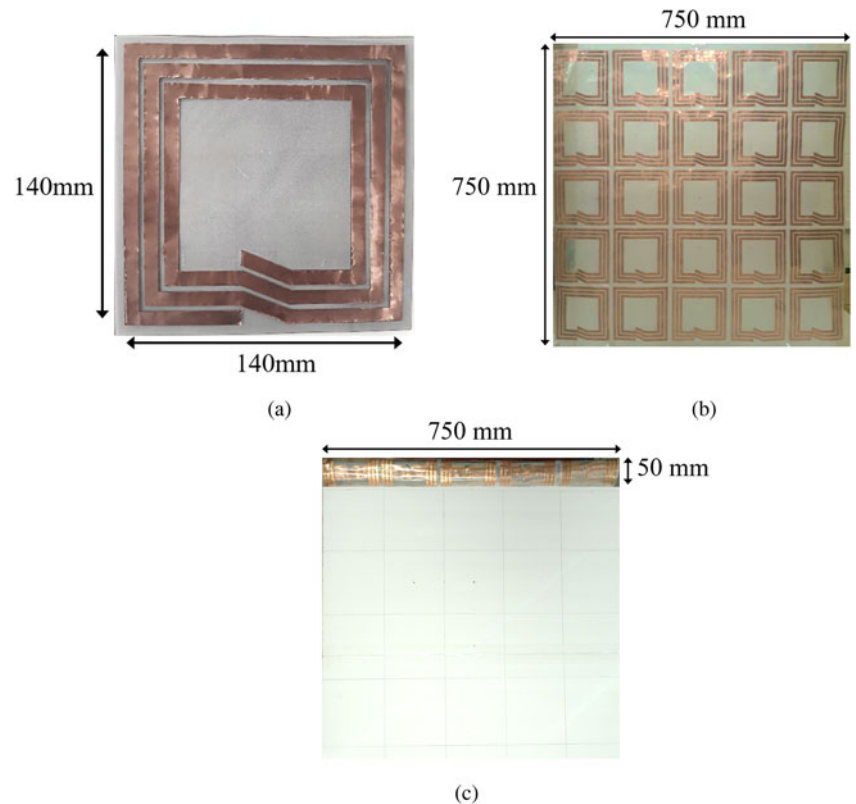
**Fig. 4.** (a) Fabricated single unit cell. (b) Fabricated rollable metamaterial screen (rolled down). (c) Fabricated rollable metamaterial screen (rolled up).
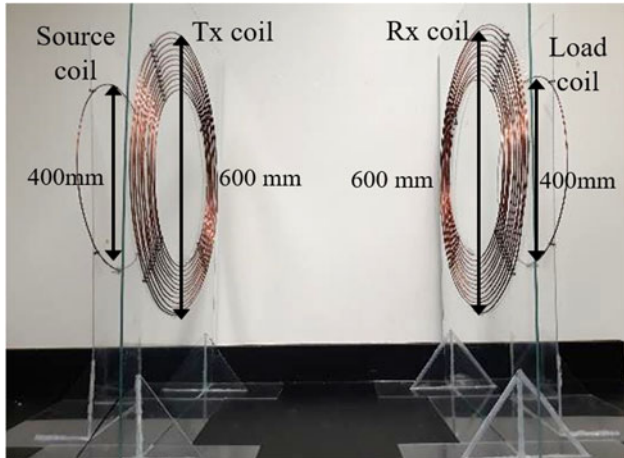


**Fig. 5.** Fabricated four-coil WPT system.

matching conditions of the WPT system should be satisfied. As for the four-coil WPT system, $Z_{IN}$ should be matched to $R_S$ using the adaptive technique [17–19] which means the distance between the source coil (load coil) and Tx coil (Rx coil) should be varied to satisfy the matching condition. The distance between Tx and Rx coils is varied in the measurements from 30 to 150 cm.

## Measurement results

### Measurements of the power transfer efficiency

The PTE of the WPT system is measured quantitatively using a vector network analyzer (HP E8361A, Agilent, Inc.), shown in

Fig. 7. The source and load coils are connected to two ports of the vector network analyzer. The magnitude of the $S$-parameter ($S_{21}$) is measured using the vector network analyzer. In case of the WPT system, the PTE is described as the ratio of the received power at the load (port 2) to the applied power at the source (port 1), so the PTE can be calculated using the following equation [19]:

$$PTE(\eta) = |S_{21}|^2 \times 100\%. \qquad (7)$$

The PTE of the WPT system is measured in an anechoic chamber which is a room designed to absorb electromagnetic waves. The anechoic chamber allows to perform the exact PTE measurement without the contribution from the reflected electromagnetic waves. We measure the PTE of the WPT system without the metamaterial screen when it is rolled up and with the metamaterial screen when it is rolled down. The rollable metamaterial screen is located in the middle between the Tx and Rx coils in order to achieve a maximum PTE. When the metamaterial screen is placed in the middle between the Tx and Rx coils, the mutual inductance between the metamaterial screen and Tx or Rx coil affects the resonant frequency of the whole WPT system. This mutual inductance causes the degradation of the PTE at the resonant frequency.

As shown in Fig. 8, there is a threshold distance (50 cm), beyond which the WPT system with the metamaterial screen shows improved PTE. The reason for that is that the mutual inductance between the metamaterial screen and Tx or Rx coil increases as the transfer distance between Tx and Rx coil decreases. Therefore, as the transfer distance decreases, the resonant frequency of the WPT system decreases but the degradation of the PTE due to the decreased resonant frequency is overcome by
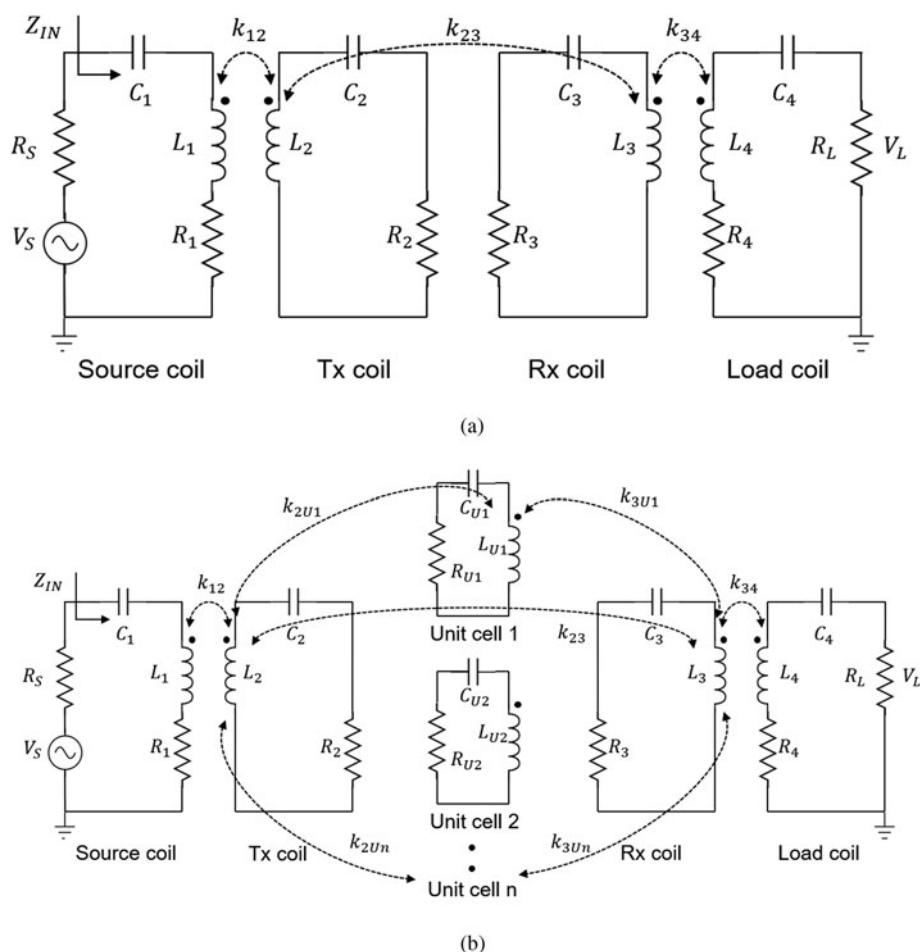
(a)

(b)

**Fig. 6.** Equivalent circuit model of: (a) four-coil WPT system without the metamaterial screen, (b) four-coil WPT system with the metamaterial screen.
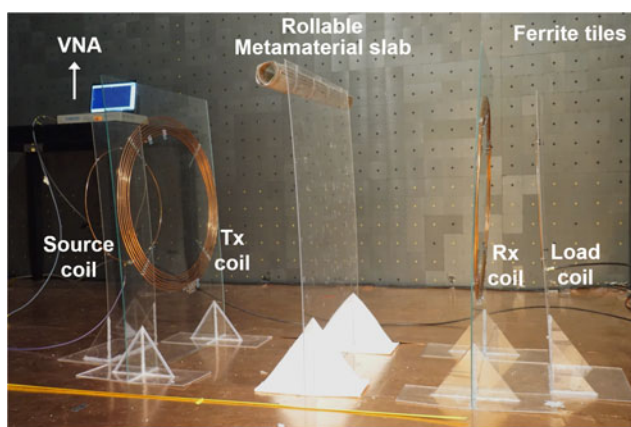


**Fig. 7.** Measurement setup for the proposed WPT system with the rollable metamaterial screen in an anechoic chamber.



**Fig. 8.** Measured PTE of the WPT system without metamaterial (rolled up) and with metamaterial (rolled down).

the increase of the PTE with metamaterial screen due to the decreased transfer distance when it becomes shorter than the threshold distance. Furthermore, for both cases with and without metamaterial screen, increase in the transfer distance results in the linear decrease of the PTE. At the transfer distance 100 cm, the PTE increases from 36 to 58.52% after the metamaterial screen is rolled down, as shown in Fig. 9(a), which is a factor of 1.63 improvements. At the distance of 150 cm, the PTE improves
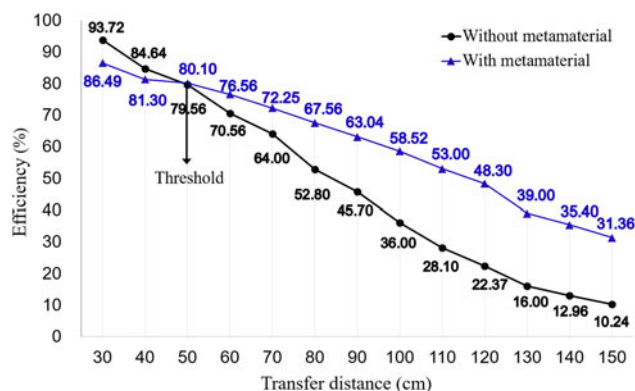
from 10.24 to 31.36% after the metamaterial screen is rolled down, as shown in Fig. 9(b), which is a factor of 3.06 improvements. Comparison of the PTE without the metamaterial screen at the transfer distance 100 cm with the PTE with the metamaterial screen at the transfer distance 140 cm shows that they are approximately the same, about 36%. It means that the transfer distance of the WPT system can be effectively increased by rolling down the rollable metamaterial screen. In addition, it is shown that there is no change when the metamaterial screen is rotated
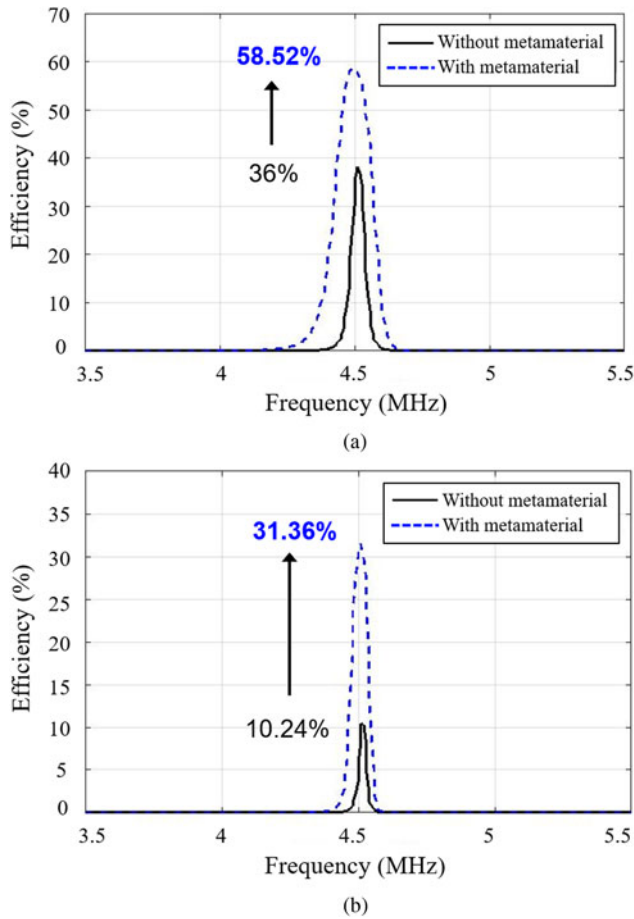
Fig. 10. Light bulb experimental setup.



Fig. 9. Comparison between the measured PTE of the system without metamaterial (rolled up) and with metamaterial (rolled down) at distances (a) 100 cm and (b) 150 cm.



Fig. 11. The intensity of the light bulb connected to the WPT system at a distance 150 cm: (a) without metamaterial, and (b) with metamaterial.

90° while keeping it parallel to Tx and Rx coils. The reason for this phenomenon is that even if the orientation of the screen is changed, the negative refractive index of the metamaterial screen is the same, resulting in the same PTE improvement. The measurement results show that the proposed rollable metamaterial screen is highly effective for increasing the PTE and the transfer distance of the WPT system.

### Light bulb experiments

The PTE of the WPT system is verified qualitatively in a light bulb experiment, where an RF power amplifier (2100L, E&I) and a function generator (33120A, HEWLETT PACKARD) are connected to the source coil, as shown in Fig. 10. An input RF power of 80 W at 4.5 MHz is provided to the source coil using the RF power amplifier and function generator. At the receiver side, a 40 W light bulb is connected to the load coil. First, the operation of the light bulb connected to the WPT system is tested at a distance 150 cm with and without the metamaterial screen. As shown in Fig. 11(a), when the metamaterial screen is not used, the light bulb does not turn on. It means that the wirelessly transferred power is not enough to turn the light bulb on, because the PTE at a distance 150 cm is 10.24%, which is quite low. However, as shown in Fig. 11(b), the light bulb turns on when the metamaterial screen is used. It means that when the PTE of
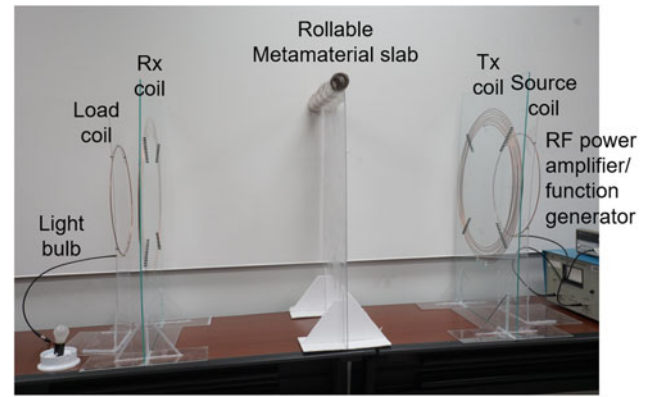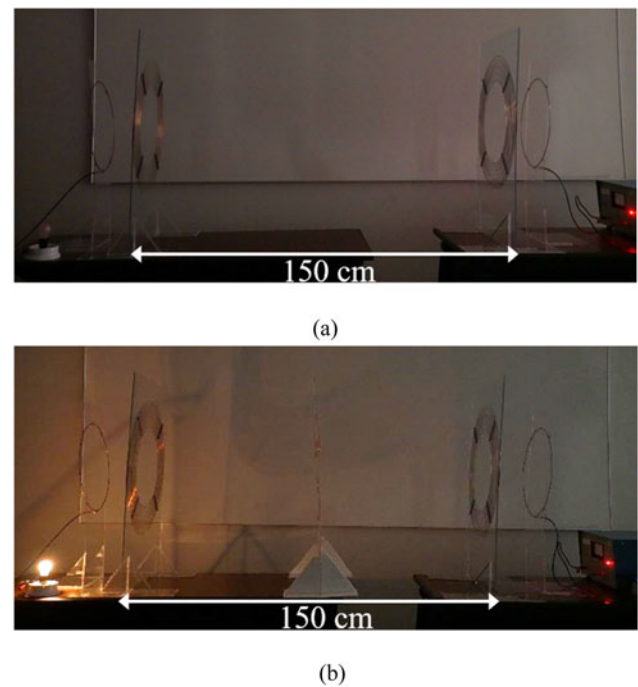
the WPT system with the metamaterial screen is 31.36%, the transferred power is high enough to turn the light bulb on.

Next, an experiment to verify the increased PTD using the metamaterial screen is performed. As shown in Figs 12(a) and 12(b), the intensity of the light bulb connected to the WPT system without the metamaterial screen at a distance of 104 cm and the intensity of the light bulb connected to the WPT system with the metamaterial screen at a distance of 155 cm are approximately the same. It means that the PTD of the WPT system is effectively increased by approximately 50 cm when the metamaterial screen is used. In addition, as shown in Fig. 8, the measured PTE without and with metamaterial screen, in Figs 12(a) and 12(b), respectively, are approximately 36 and 31.36%, respectively. The measured PTEs are approximately the same, which means that the results of the quantitative PTE measurement and the qualitative light bulb experiments are well matched to each other.
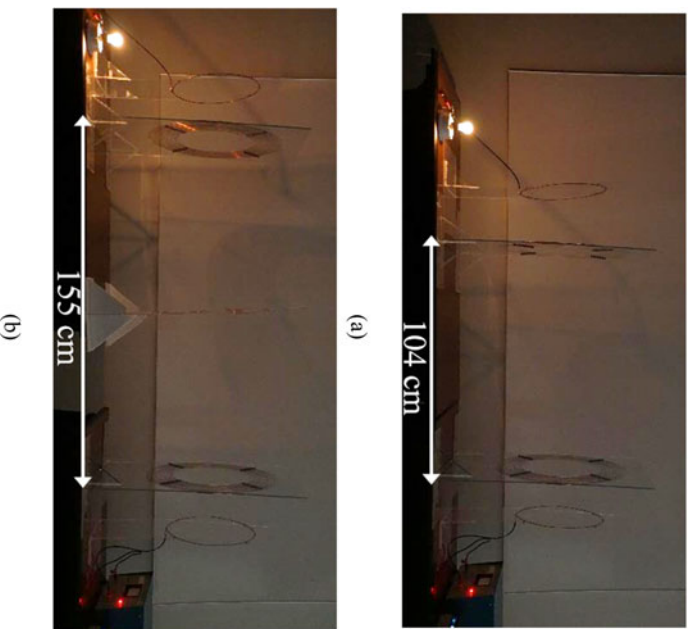
**Fig. 12.** The intensity of the light bulb connected to the WPT system: (a) at a distance 104 cm without metamaterial, and (b) at a distance 155 cm with metamaterial.
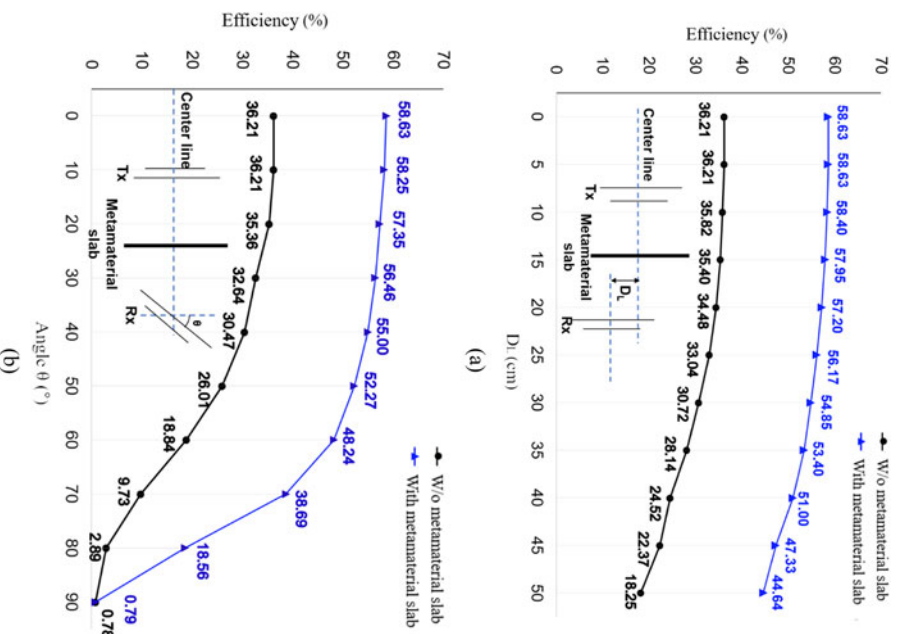


**Fig. 13.** Measured PTE of the WPT system with: (a) lateral misalignment ($D_L$), (b) angular misalignment (θ) at 100 cm.

**Table 1.** Comparison of the rollable metamaterial screen with earlier reported metamaterial (MTM) based WPT systems

| Ref. | Operating frequency (MHz) | Diameter of Tx/Rx coils (mm) | Negative refraction index | Configuration of the MTM | Transfer distance (mm) | Normalized transfer distance | Thickness of the MTM slab (mm) | Flexibility/ rollability | Efficiency with MTM (%) |
|---|---|---|---|---|---|---|---|---|---|
| [3] | 27 | 400 | $\mu_r = -1$ | Double sided with via | 500 | 2.5 | 1.64 | × | 47 |
| [4] | 6.5 | 600 | Negative $\mu_r$ | Single sided | 900 | 3 | 1.2 | × | 50 |
| [4] | 6.5 | 600 | Negative $\mu_r$ | Single sided, 3D structure | 900 | 3 | 150 | × | 54 |
| [5] | 7.43 | 150 | $\mu_r = 0$ $\mu_r = -1$ | Double sided with via | 250 | 2.67 | 1.6 | × | 18.6 |
| [20] | 26.65 | Tx = 50 Rx = 36 | $\mu_r = -1$ | Double sided | 50 | 2 | 19 | × | 18.23 |
| [21] | 5.57 | 40 | $\mu_r = -1$ | 3D structure | 40 | 2 | 26 | × | 35 |
| This work | 4.5 | 600 | $\mu_r = -1$ | Single sided | 900 | 3 | 0.16 | ○ | 63.04 |

### PTE measurement of the misaligned WPT

The effects of the misalignments between Tx and Rx coils are also investigated. In practical applications, the exact alignment between the transmitter and receiver coils is a very challenging task. Obviously, the misalignments in the WPT system degrade its performance. The lateral and angular misalignment on the PTE of the WPT system with and without the rollable metamaterial screen at a distance 100 cm is studied. As shown in Fig. 13(a), when the misaligned lateral distance ($D_L$) increases, the PTE decreases for both cases (with and without the metamaterial screen). However, when the metamaterial screen is rolled down, the PTE increases by 20–25% at all distances. The results of measurements at the angular misalignment ($\theta$) are shown in Fig. 13(b). The PTE of the WPT system with and without the rollable metamaterial screen decreases when the angular misalignment of the Rx coil increases. It is noticeable that the effects of the rollable metamaterial screen on the PTE decrease as the angular misalignment increase. Especially, the improved PTE is almost 0% at the angle of 90°. It means that the magnetic field generated by the Tx coil does not cross-link the Rx coil when the Rx coil is perpendicular to the direction of the magnetic field even though the magnetic field is focused by the metamaterial screen. However, in all other cases, it is proved that the rollable metamaterial screen compensates the effects of the misalignments in the WPT system.

### Measurement comparison

The WPT system with the rollable metamaterial screen is compared in Table 1 with the performance of previously reported metamaterial-based WPT system. For the comparison purpose, the transfer distance between Tx and Rx is normalized to the radius of the Tx coil because of the different coil sizes. The equation for the normalized transfer distance is as follows [4]:

$$\text{Normalized transfer distance} = \frac{\text{Transfer distance}}{\text{Radius of the Tx}}. \tag{8}$$

It is observed that the use of a thin metal layer and flexible substrate reduces the design complexity, as well as the power losses within the metamaterial screen. The comparably low loss tangent ($\delta \cong 0.0003$ at 1 MHz) and very thin thickness (0.0762 mm) of the polyethylene substrate lead to the low dielectric loss of the substrate. In addition, a simple square spiral resonator structure has advantages in terms of $Q$-factor over split-ring resonator structure [13], which results in a higher PTE. These factors allow the WPT system with the rollable metamaterial screen to have a substantially improved PTE as compared with the one described in the previous work. Moreover, the metamaterial screen has flexibility and rollability because of its extremely thin metamaterial structure which enables the consumers to utilize the space occupied by the metamaterial screen when it is rolled up.

### Conclusion

This paper demonstrates the use of a rollable metamaterial screen in high-efficient MRC WPT system. The rollable metamaterial screen has a very thin structure with very low power losses and excellent rollability, resulting in compactness and portability. The PTE of the WPT system can be effectively enhanced by the metamaterial screen capability to focus magnetic field.

Moreover, the WPT system with the rollable metamaterial screen uses the space effectively, i.e. the screen is rolled down only if it is needed. The PTE of the WPT system with rollable metamaterial screen increases from 36 to 58.52% at 100 cm, and from 10.24 to 31.36% at 150 cm. The quantitative measured PTE values are well matched to the qualitative light bulb experimental results. The lateral and angular misalignments in the WPT system are also studied. The results show that the rollable metamaterial screen improves the PTE at misaligned condition by such a way that the rollable metamaterial screen compensates the effects of the misalignments. It is expected that the rollable metamaterial screen of the high-efficiency WPT system will introduce new possibilities for practical application in the electronic charging devices with increased portability and space usage.

### References

1. **Tesla N.** Apparatus for transmitting electrical energy, US Patent, 1119732, Dec. 1914, No. 371817.
2. **Kurs A, Moffatt R and Soljačić M** (2010) Simultaneous mid-range power transfer to multiple devices. *Applied Physics Letters* **96**, Art. no. 044102, 044102.1–044102.3.
3. **Wang B, Teo KH, Nishino T, Yerazunis W, Barnwell J and Zhang J** (2011) Experiments on wireless power transfer with metamaterials. *Applied Physics Letters* **98**, Art. no. 254101, 254101.1–254101.3.
4. **Ranaweera ALAK, Duong TP and Lee JW** (2014) Experimental investigation of compact metamaterial for high efficiency mid-range wireless power transfer applications. *Journal of Applied Physics* **116**, 043914.1–043914.8.
5. **Cho Y, Lee S, Kim DH, Kim H, Song C, Kong S, Park J, Seo C and Kim J** (2018) Thin hybrid metamaterial slab with negative and zero permeability for high efficiency and low electromagnetic field in wireless power transfer systems. *IEEE Transactions on Electromagnetic Compatibility* **60**, 1001–1009.
6. **Shaw T and Mitra D** (2019) Wireless power transfer system based on magnetic dipole coupling with high permittivity metamaterials. *IEEE Antennas and Wireless Propagation Letters* **18**, 1823–1827.
7. **Smith DR, Schurig D, Mock JJ, Kolinko P and Rye P** (2004) Partial focusing of radiation by a slab of indefinite media. *Applied Physics Letters* **84**, 2244–2246.
8. **Maslovski S, Tretyakov S and Alitalo P** (2004) Near-field enhancement and imaging in double planar polariton-resonant structures. *Journal of Applied Physics* **96**, 1293–1300.
9. **Padilla WJ, Basov DN and Smith DR** (2006) Negative refractive index metamaterials. *Materials Today* **9**, 28–35.
10. **Veselago V** (1968) The electrodynamics of substances with simultaneously negative values of $\varepsilon$ and $\mu$. *Soviet Physics-Uspekhi* **10**, 509–514.
11. **Pendry JB** (2000) Negative refraction makes a perfect lens. *Physical Review Letters* **85**, 3966.
12. **Urzhumov Y and Smith DR** (2011) Metamaterial-enhanced coupling between magnetic dipoles for efficient wireless power transfer. *Physical Review B* **83**, 205114.
13. **Hao T, Stevens CJ and Edwards DJ** (2005) Optimization of metamaterials by Q factor. *Electronics Letters* **41**, 653.
14. **Smith D, Schultz S, Markos P and Soukoulis C** (2002) Determination of effective permittivity and permeability of metamaterials from reflection and transmission coefficients. *Physical Review B: Condensed Matter and Materials* **65**, Art. no. 195104, 195104.1–195104.5.
15. **Smith D, Vier D, Koschny T and Soukoulis C** (2005) Electromagnetic parameter retrieval from inhomogeneous metamaterials. *Physical Review E: Statistical Physics, Plasmas, Fluids, and Related Interdisciplinary Topics* **71**, Art. no. 036617, 036617.1–036617.11.

16. **Chen X, Grzegorczyk TM, Wu B-I, Pacheco Jr J and Kong JA** (2004) Robust method to retrieve the constitutive effective parameters of metamaterials. *Physical Review E: Statistical Physics, Plasmas, Fluids, and Related Interdisciplinary Topics* **70**, Art. no. 016608, 016608.1–016608.7.
17. **Hoang H, Lee S, Kim Y, Choi Y and Bien F** (2012) An adaptive technique to improve wireless power transfer for consumer electronics. *IEEE Transactions on Consumer Electronics* **58**, 327–332.
18. **Sample AP, Meyer DA and Smith JR** (2011) Analysis, experimental results, and range adaption of magnetically coupled resonators for wireless power transfer. *IEEE Transactions on Industrial Electronics* **58**, 544–554.
19. **Duong TP and Lee JW** (2011) Experimental results of high-efficiency resonant coupling wireless power transfer using a variable couple method. *IEEE Microwave and Wireless Components Letters* **21**, 442–444.
20. **Rajagopalan A, RamRakhyani AK, Schurig D and Lazzi G** (2014) Improving power transfer efficiency of a short-range telemetry system using compact metamaterials. *IEEE Transactions on Microwave Theory and Techniques* **62**, 947–955.
21. **Rodríguez ESG, RamRakhyani AK, Schurig D and Lazzi G** (2016) Compact low-frequency metamaterial design for wireless power transfer efficiency enhancement. *IEEE Transactions on Microwave Theory and Techniques* **64**, 1644–1654.

**Woosol Lee** received the B.S. degree from the Korea Military Academy, Seoul, Korea in 2011, and the M.S. degree from the Ajou University, Suwon, Korea, in 2016. He is currently pursuing the Ph.D. degree in electrical and computer engineering at the University of Florida, Gainesville, FL, USA. His current research interests include metamaterials for RF/microwave applications, wireless power transfer, RF passive components designing, and low-loss conductors for high-frequency applications.
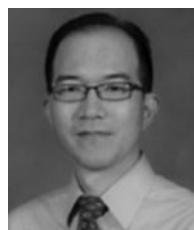
**Yong-Kyu Yoon** received the Ph.D. degree in electrical and computer engineering from the Georgia Institute of Technology, Atlanta, GA, USA in 2004. He held a Post-Doctoral Researcher position with the Georgia Institute of Technology, from 2004 to 2006. He was an Assistant Professor in the Department of Electrical Engineering, State University of New York, Buffalo, NY, USA, from 2006 to 2010. He joined the University of Florida, Gainesville, FL, USA, as an associate professor in 2010. He is currently a Professor and graduate coordinator in the Department of Electrical and Computer Engineering at UF. He spent his sabbatical leave at Seoul National University, from July and December 2017. He has authored over 200 peer-reviewed publications. His current research interests include microelectromechanical systems, nanofabrication, and energy storage devices; metamaterials for RF/microwave applications; micromachined millimeter-wave/terahertz antennas and waveguides; wireless power transfer and telemetry systems; lab-on-a-chip devices; and ferroelectric materials for memory and tunable RF devices. He was a recipient of the NSF Early Career Development Award in 2008 and the SUNY Young Investigator Award in 2009.